RSC Advances

ROYAL SOCIETY OF CHEMISTRY

www.rsc.org/advances

PCL-F68-PCL/PLGA-PEG-PLGA mixed micelles mediated delivery of mitoxantrone for reversing multidrug resistant in breast cancer

Yuee Cai[1], Shengpeng Wang[1], Minghui Wu[2], Jonathan K. Tsosie[3], Xi Xie[4], Jianbo Wan[1], Chengwei He[1], Huayu Tian[5], Xuesi Chen[5], Meiwan Chen[1]*

[1]State Key Laboratory of Quality Research in Chinese Medicine, Institute of Chinese Medical Sciences, University of Macau, Taipa 999078, Macau, China

[2] Department of Cell Biology and Anatomy, College of Medicine, University of Florida, Gainesville, Florida, USA, 32601

[3] New Mexico Institute of Mining and Technology, Socorro, New Mexico, 87801

[4] School of Chemistry and Chemical Engineering, Sun Yat-Sen University, Guangzhou, China, 510275

[5] Key Laboratory of Polymer Ecomaterials, Changchun Institute of Applied Chemistry, Chinese Academy of Sciences, Changchun, China, 130022

***Correspondence Authors**

Dr. Meiwan Chen, Institute of Chinese Medical Sciences, University of Macau, Av. Padre Tomas Pereira S.J., Taipa, Macau, China

E-mail: mwchen@umac.mo

Mitoxantrone (MIT) is a promising candidate for cancer therapy, but the clinical application of MIT against cancers was hindered by its multidrug resistance (MDR) effect, which has drawn much attention. Herein, amphihilic poly(ε–caprolactone)-pluronic F68-poly(ε–caprolactone) (PFP) and PLGA-PEG-PLGA(PPP) polymers are designed to fabricate mixed micelles for the efficient delivery of MIT with reversed effect of MDR. These mixed micelles (MIT-PFP/PPP micelles) exerted favorable particle size of 144.70 ± 10.52 nm and encapsulation efficiency of 56.69% ± 4.67. Importantly, MIT-PFP/PPP micelles could strongly inhibit cell proliferation in MCF-7/ADR cells with the IC_{50} of 3.503±0.163 μM for 24 h, which was about 7.7-fold lower than that of free MIT. The molecular mechanism of reversed MDR effect in MCF-7/ADR cells is ascribed to the downregulation of P-glycoprotein (P-gp) by MIT-PFP/PPP micelles resulting in enhanced anticancer efficacy. These findings suggest that MIT-PFP/PPP micelles have great potential for the overcome of MDR effect by inhibiting the protein expression of P-gp in cancer cells.

1. Introduction

Mitoxantrone (MIT), an anthracenedione developed as a doxorubicin analogue, has been recognized as an antineoplastic agent by U.S. Food and Drug Administration (FDA).[1, 2] It is reported that MIT has antitumor activity in various cancers, including breast cancer, prostate cancer, lymphomas and acute leukemia.[3-5] However, the application of MIT is restricted by the development of multidrug resistance (MDR) during the treatment associated with the overexpress level of adenosine triphosphate-binding cassette (ABC) transporters like P-glycoprotein (P-gp)，resulting in non-ideal anticancer efficacy.[6] Therefore, it still remains a primary challenge to enhanced anticancer efficacy of MIT against cancers with MDR during chemotherapy. To conquer MDR, diverse strategies are employed, such as analogs of chemotherapeutic agents,[7] prodrugs,[8] P-gp specific antibodies [9] and polymeric micelles.[10] Among these, polymeric micelles are able to encapsulate hydrophobic drugs by core-shell structure, exhibit enhanced permeability and retention (EPR) effect with suitable particle size [11] and some of them function as biological response modifiers against MDR, such as pluronic block copolymers.[12]

Pluronic, also known as Poloxamers, are applied as a polymeric backbone to form micelles [13] and pluronic F68 (F68) has been approved for intravenous injection by US Food and Drug Administration (FDA).[14] Poly(ε–caprolactone) (PCL) is used as the hydrophobic segment of amphiphilic copolymers with less degradation products and high permeability to drugs,[15] which may be suitable to decorated with F68 for better efficiency of its drug delivery system. Moreover, the characteristics of polymeric micelles, including particle size, encapsulation efficiency and drug loading, still need to be improved by applying mixed micelle formulation.[16, 17] Thus, poly(D,L-lactide-co-glycolide)-poly(ethylene glycol)-poly(D,L-lactide-co-glycolide) (PLGA-PEG-PLGA), which has become a promising polymer in the application of pharmaceutics due to its biodegradability, acceptable bioavailability and sustained drug release profile, was applied in the formation of mixed micelles in this study.[18]

Herein, PCL-F68-PCL (PFP)/PLGA-PEG-PLGA (PPP) mixed micelle system (PFP/PPP micelles) has been shown to deliver MIT against MDR in human breast

cancer cell line (MCF-7/ADR cells) in this study. Firstly, PFP was synthesized by esterification between F68 and PCL to form an amphiphilic copolymer used in the mixed micelle system and the structure of synthesized PFP was confirmed by nuclear magnetic resonance spectroscopy (^{1}H NMR) and fourier transform infrared spectroscopy (FTIR). Secondly, the mass ratio of PFP and PPP was investigated from 1:4 to 4:1 and then the optimized mass ratio (1: 2) was determined. The mixed micelle system (MIT-PFP/PPP micelles) exerted favorable particle size of 144.70 ± 10.52 nm determined by dynamic light scattering (DLS) and encapsulation efficiency of 56.69% ± 4.67. The critical micelle concentration (CMC), in vitro drug release profile and stability were also measured. Thirdly, the mixed micelle system (MIT-PFP/PPP micelles) showed suitable biocompatibility and enhanced cellular uptake as well as cytotoxicity on MCF-7/ADR cells through anti-proliferation effect and inhibition of P-glycoprotein instead of apoptotic effect confirmed by 3-(4,5-dimethyl-2-thiazolyl)-2,5-diphenyl tetrazolium bromide (MTT) assay, nuclear staining, cell apoptosis and western blot analysis.

2. Materials and methods

2.1 Materials

Pluronic F68 (F68) was purchased form BASF SE (Ludwigshafen, German). Poly(ε–caprolactone) (PCL, MW 3500) and $PLGA_{5600}$-PEG_{2000}-$PLGA_{5600}$ (PPP) were purchased from Daigang Biomaterial (Jinan, China). 4-Dimethylaminopyridine (DMAP) and dicyclohexylcarbodiimide (DCC) were obtained from GL Biochem (Shanghai, China). Mitoxantrone (MIT) (98% purity) was purchase from Meilun Biology Technology Company (Dalian, China). Fetal bovine serum (FBS), Dulbecco's Modified Eagle Medium (DMEM), phosphate-buffered saline (PBS), penicillin-streptomycin (PS), propidium iodide (PI) and 0.25% trypsin/1 mM ethylene diamine tetraacetic acid (EDTA) (w/v) were purchased from Life Technologies (Grand Island, USA). 3-(4, 5-dimethyl-2-thiazolyl)-2, 5-diphenyl tetrazolium bromide (MTT) and Hoechst 33342 were purchased from Sigma Aldrich (St. Louis, MO, USA). The primary antibodies against GADPH and P-gp were acquired from Cell

Signaling Technology (Boston, USA). All chemicals were in analytical grade. Water was ultrafiltered via a Milli-Q apparatus (Millipore, Billerica, MA, USA).

2.2 Cell lines and cell culture

Human breast carcinoma Michigan Cancer Foundation-7 cell (MCF-7) was acquired from the American Type Culture Collection (ATCC). Doxorubicin-resistant MCF-7 cell (MCF-7/ADR) was selected by stepwise increasing the concentrations of doxorubicin as described previously.[19] Both MCF-7 and MCF-7/ADR cells were cultured in DMEM medium with 100 U/ml penicillin, 100 μg/ml streptomycin and 10% FBS (v/v) under 5% CO_2 at 37ºC.

2.3 Synthesis and characterization of PCL-F68-PCL

PCL-F68-PCL (PFP) was synthesized by the esterification between the hydroxyl group of F68 and the carboxyl group of PCL. Briefly, F68 (0.02 mM), PCL (0.06 mM), DMAP (0.02 mM), DCC (0.06 mM) were dissolved in dimethyl sulphoxide (DMSO) (10 mL) and stirred for 36 h at 25℃. 500 mL DMSO was used to remove the unreacted materials and byproducts via dialysis for 12 h. Then the dialysis bag was transferred into pure water to remove the DMSO for 48 h. Lastly, the solution in the dialysis bag was collected for 48 h by freeze-drying.

^{1}H NMR and FTIR were used to confirm the structure of PFP after synthesis. The ^{1}H NMR spectroscopy (Bruker, Karlsruhe, Germany) analysis was done using deuterated chloroform at 400 MHz. The F68 or PFP was mixed with KBr and scanned by a NEXUS 670 FTIR spectrophotometer (Nicolet, Hudson, NH) at a spectrum range of 400-4000 cm^{-1}.

2.4 Preparation and characterization of mixed micelles

2.4.1 Preparation of mixed micelles in different ratios

MIT loaded PFP/PPP mixed micelles (MIT-PFP/PPP micelles) were prepared by solvent evaporation as reported previously.[20] Fourteen mg copolymers with different mass ratios of PFP and PPP were mixed with 1 mg MIT. The mixtures were then

dissolved in water miscible organic solvent (800 μl) of methanol and acetonitrile (1:1, v/v) under ultrasonication. When the copolymers were completely dissolved, the mixed solution was added drop-wise into pure water and stirred for 5 h until the methanol and acetonitrile were evaporated. The final solution was filtered using a 0.45 μM Millipore filter to remove any large aggregate. Filtration isolated MIT-PFP/PPP micelles with particle size less than 450 nm. The whole procedure was performed in a dark room.

2.4.2 Characterization of mixed micelles

MIT encapsulated micelles with various mass ratios of PFP/PPP were analyzed based on their particle size and morphology. The optimum ratio of MIT-PFP/PPP was established from the cytotoxicity of blank materials. The particle size was detected by dynamic light scattering (DLS) at 25ºC with a ZetasizerNano ZSP system (Malvern Instrument, Worecestershire, UK). Micelle morphology was determined by transmission electron microscopy (TEM, Tecnai G20, FEI Company, Oregon, USA). Micelle samples were deposited on a carbon-coated copper grid and stained with the solution of phosphotungstic acid (2%, w/v) for 30 s. TEM images were examined at 200 kV.

2.4.3 Encapsulation efficiency and drug loading

The drug concentration of MIT-PPP micelles and MIT-PFP/PPP micelles was measured by Waters e2695 HPLC with a C18 reverse-phase liquid chromatography column (250 mm × 4.6 mm) at a flow rate of 1 mL/min and maximum absorption wavelength of 609 nm. The mobile phase consisted of methanol/0.25% acetic acid (50/50, v/v). Methanol was added to the MIT-PFP/PPP micelle solution to destroy the core-shell structure, resulting in the release of MIT. The EE% and DL% were obtained by the following equation:[21]

$$EE\% = \frac{\text{Weight of encapsulated drug}}{\text{Weight of feeding drug}} \times 100\% \quad (1)$$

$$DL\% = \frac{\text{Weight of encapsulated drug}}{\text{Weight of feeding drug + Weight of polymers}} \times 100\% \quad (2)$$

2.4.4 Critical micelle concentration and stability of mixed micelles

The critical micelle concentration (CMC) of blank PFP/PPP micelles was measured by a Lumina Fluorescence spectrometer (Thermo Scientific) using pyrene as the fluorescence probe.[22-24] A series of blank PFP/PPP micelles with various concentration ranging from 5×10^{-9} to 1.4 mg/mL were prepared in the presence of pyrene (7×10^{-7} M). The spectra were recorded from 350 to 450 nm with an excitation wavelength of 339 nm. The fluorescence intensity ratio of the first and the third vibronic peaks (I_{373}/I_{384}) was determined by the polarity of the pyrene environment, aggregation number, and core cavity. The ratio of I_{373}/I_{384} decreased as the environment of the pyrene was becoming more hydrophobic, indicating that micelles are not capable of encapsulating pyrene. The CMC value was obtained from the intersection of both horizontal and inflection point tangents. In addition, a study based on a well-known phenomenon of Tyndall was used to evaluate the micellization ability of blank PFP/PPP micelles. Briefly, various concentrations of blank PFP/PPP micelles ranging from 1.4 to 1.4×10^{-4} were prepared and then were irradiated by a red laser pointer to observe the Tyndall phenomenon.

The stability of MIT-PFP/PPP micelles was investigated by examining changes of the mean particle size when MIT-PFP/PPP micelles were mixed with different concentrations of FBS solution.[25] MIT-PFP/PPP micelles dispersed in water with 10%, 20%, 30% and 40% of FBS were incubated at 37℃ for 24 h. At pre-determined time points (0 h, 1 h, 2 h, 4 h, 8 h, 12 h and 24 h), the average particle size of MIT-PFP/PPP micelles was measured by DLS. The diameter ratio was the ratio between the hydrodynamic diameter at different time points and its initial diameter in water.

2.5 *In vitro* release of MIT from mixed micelles

The *in vitro* release of MIT from MIT-PFP/PPP micelles was determined by utilizing a dialysis bag (molecular weight cutoff of 10000 Da) under sink condition. Two mL of MIT-PFP/PPP micelles was added into a dialysis bag immersed in 30 mL of fresh PBS solution (pH 7.4, 0.1 M) containing 0.1% Tween 80 (v/v) and then the bag was placed in a shaking incubator with stirring at the speed of 100 rpm at 37℃. The *in vitro* drug release of MIT from MIT-PPP micelles was investigated using the same method. Additionally, MIT was dissolved in methanol due to its poor water solubility and used as a control for the *in vitro* drug release profile. The MIT control solution was analyzed using the same method mentioned above. One mL fresh medium was used to refill the dialysis bags after 1 mL medium was released in order to maintain the initial volume. The concentration of MIT released from micelles was measured by HPLC as mentioned above. The kinetic release profile of MIT was analyzed by the following equation:[26]

$$M_i = C_i \times 30\ mL + \sum_{j=1}^{j=i-1} C_j \times 1\ mL,$$

$$\text{Cumulative release } (\%) = \frac{M_i}{M_A} \times 100\%. \qquad (3)$$

Where Mi is the amount of the drug released at the time point, i. Ci represents the concentration of MIT (mg/mL) from the collected release medium at the time point, i. Cj represents the total amount of MIT in the collected release medium before the time point, j. MA represents the initial amount of MIT in the dialysis bags.

2.6 *In vitro* cytotoxicity study

The cytotoxicity of blank materials and mixed-ratio micelles against MCF-7 and MCF-7/ADR cells was determined using a MTT assay.[27] The cells were seeded in 96-well plates in 100 μL medium at the density of 5.0×10^3 cells/well and then incubated for 24 h. The cells were incubated with free MIT, MIT-PPP micelles and MIT-PFP/PPP micelles at different concentrations ranging from 0.125 μM to 2 μM,

while blank materials of PFP, PPP, PFP/PPP (1: 2) were added to the cells at various concentrations ranging from 12.5 μg/mL to 400 μg/mL. After 24 h or 48 h incubation at 37℃, 20 μL of MTT dye (5 mg/mL) was used to replace the medium for another 4 h of incubation to form formazan crystals by mitochondrial dehydrogenases, which was followed by dissolving formazan crystals by DMSO. The spectrophotometric absorbance at 570 nm was recorded by a microplate reader (SpectraMax M5, Molecular Devices, USA). The results were analyzed to demonstrate relative cell viability.

2.7 Cellular uptake study

The cellular uptake of mixed micelles was determined by flow cytometry (BD FACS Canto^{TM}, BD Biosciences, San Jose, CA, USA). MCF-7 and MCF-7/ADR cells were seeded on 12-well culture plates at the density of 2×10^5 cells/well and cultured for 24 h. Then free MIT, MIT-PPP micelles and MIT-PFP/PPP micelles were added into the cells with an equivalent concentration of 2 μM MIT followed by incubation for another 3 h, 6 h, and 12 h respectively. Afterwards, the cells were collected and washed twice with ice-cold PBS (pH 7.4). Lastly, the cells were resuspended with 0.5 mL PBS and analyzed with flow cytometry.

2.8 Nuclear morphology

Hoechst staining assay was used to examine chromosome condensation and nuclear morphological changes of MCF-7/ADR cells seeded in 96-well plates at a density of 5×10^3 cells/well. Cells were treated with free MIT, MIT-PPP micelles and MIT-PFP/PPP micelles at an equivalent concentration of 2 μM MIT. After incubation for 48 h, 4% paraformaldehyde was used to fix the cells. The cells were then washed with PBS and stained with Hoechst 33342 (1 μg/mL) at 25℃. The stained cells were visualized and imaged by using Incell Analyzer 2000 (GE Healthcare Life Sciences, USA) equipped with DAPI filter (excitation 350 nm and emission 455 nm).

2.9 Cell apoptosis analysis

Apoptotic cells were measured by an Annexin V/PI apoptosis detection kit (BioVision) following the manufacturer's instruction. MCF-7/ADR cells were seeded in 6-well plates and cultured for 24 h. Then, free MIT, MIT-PPP micelles and MIT-PFP/PPP micelles were treated to the cells with an equivalent concentration of 2 μM MIT. After incubation for 48 h, the cells were collected and washed twice with cold PBS. The cells were then gently suspended in 100 μL of binding buffer and stained with 5 μL of Annexin-FITC and 10 μL solution of PI followed by incubation in the dark for 15 mins at 25℃. Cell apoptosis was then analyzed by flow cytometry.

2.10 Western blot analysis

Western blotting was used to analyze specific proteins as previously reported.[28] Free MIT, MIT-PPP micelles and MIT-PFP/PPP micelles were used to treat MCF-7 and MCF-7/ADR cells with an equal concentration of 2 μM MIT after 48 h. The total cellular protein was collected using a RIPA lysis buffer containing a 1% protease inhibitor cocktail and 1% phenylmethanesulfonylfluoride (PMSF). The concentrations of protein were measured using a BCA protein assay kit (Thermo Scientific). 10% Sodium dodecylsulfate polyacrylamide gel electrophoresis (SDS-PAGE) was used to separate proteins before the proteins were transferred to polyvinylidene fluoride (PVDF) membranes. After being blocked with 5% non-fat dried milk for 1 h, the membranes were incubated with specific primary antibodies against GADPH and P-gp (1:1000) followed by incubation with the corresponding secondary rabbit antibodies (1:1000). The specific protein bands were visualized by an ECL Advanced Western Blotting Detection kit (GE Healthcare Life Sciences) and imaged by film development.

2.11 Statistical analysis

Statistical analysis was done using GraphPad Prism 5 software (GraphPad Software, San Diego, CA, USA). The results were represented as the mean of arbitrary values ± standard deviation. A p value less than 0.05 was considered as statistically significant.

3. Results and discussion

3.1 Characterizations of PFP

The synthesis of the PFP copolymer is illustrated in Fig. 1A. The PFP copolymer was used to fabricate MIT-PFP/PPP micelles. Briefly, the hydroxyl group of F68 reacted with carboxyl group of PCL via esterification in order to enhance encapsulation of hydrophobic drugs. The chemical structure of PCL-F68-PCL was confirmed by ^{1}H NMR spectroscopy (Fig. 1B). A strong signal was detected at 3.66 ppm and identified as the -CH_2 group (a) of PEO, and the peaks shown at 1.17, 3.42 and 3.57 ppm were identified as -CH_3 (b), -CH (d) and -CH_2 groups (c) of PPO in F68 respectively. Meanwhile, the typical signals of PCL were observed, including peak e (δ = 2.394 ppm for -CH_2), f and g (δ = 1.5-2.0 ppm for -CH_2), h (δ = 4.11 ppm for -CH_2) and i (δ = 1.279 ppm for -CH_2). Additionally, FTIR spectroscopy was used to further validate PCL-F68-PCL synthesis (Fig. 1C). The stretching vibration peaks at 3500 and 2896 cm^{-1} were attributed to the -OH and -CH_3 groups in F68, respectively. A wide stretching peak at 3509 cm^{-1} was attributed to be the -OH and -COOH groups from PCL and the stretching peak of the -CH_2 group in PCL was present at 2940 cm^{-1}. The peak at 1723 cm^{-1} was attributed to be the C=O stretching mode of ester in PCL. Thus, the stretching peaks at 3465 cm^{-1}, 2940 cm^{-1}, 2896 cm^{-1}, 1723 cm^{-1} were recognized as the -OH and -COOH, -CH_3, -CH_2, C=O groups from PCL-F68-PCL respectively. Taken together, the ^{1}H NMR and FTIR spectra demonstrated the successful synthesis of the PFP copolymer.

3.2 Characterizations of mixed micelles

The location of drug accumulation in the human body is highly dependent on micelle particle size. It was reported that nanoparticles larger than 200 nm and less than 1 μm are easily filtered out in the spleen, while particle sizes ranging between 10 and 200 nm could facilitate drug accumulation in tumors via EPR effect.[29, 30] In this study, the average particle size and particle dispersion index (PDI) of MIT-PFP/PPP micelles varied with different ratios of PFP and PPP from 1: 4 to 4: 1. As shown in Fig. 1D, the sizes of MIT-PPP micelles (0: 1) and MIT PFP micelles (1: 0) were both above 150

nm, while the sizes of mixed micelles were less than 150 nm with the exception of the mixed micelles with the ratio of 1:4. Additionally, MIT-PFP/PPP micelles with the ratio of 1: 2 demonstrated a lower PDI of 0.086 ± 0.009 than other ratios and presented an ideal average particle size of 144.70 ± 10.52 nm (shown in Fig. 2A). Furthermore, the cytotoxicity of blank materials including PFP, PPP and PFP/PPP (1:2) in MCF-7 and MCF-7/ADR cells was measured and is shown in Fig. 2E. The results suggested that PFP/PPP (1:2) had less cytotoxicity than pure PFP and PPP in both MCF-7 and MCF-7/ADR cells, indicating the formulation contains a low ratio of PFP and has a reasonable average particle size synomonous with its biocompatibility. Thus, MIT-PFP/PPP micelles with the ratio of 1: 2 were shown to provide the optimal particle size, PDI and biocompatibility. The average particle size of blank PFP/PPP (1:2) micelles were 152.66 ± 9.87 nm, shown in Fig. 2B.

In addition to the particle size, the shape of MIT-PFP/PPP micelles also plays an important role in delivery. Morphology was observed using TEM and shown in Fig. 2C. The MIT-PFP/PPP micelles were slightly smaller than the average particle size tested via DLS, likely due to dehydration caused during preparation.[13] The average EE% of MIT-PPP micelles and MIT-PFP/PPP micelles were 42.97% ± 1.54 and 56.69% ± 4.67, respectively. The average DL% of MIT-PFP/PPP micelles was 4.11% ± 0.61, which was slightly higher than that of MIT-PPP micelles (3.86% ± 0.11).

CMC is a typical parameter used to reflect the self-assemble stability of micelles.[31] The CMC of blank PFP/PPP micelles was 0.000158 mg/mL, as shown in Fig. 3A, indicating that blank PFP/PPP micelles maintain strong thermodynamic stability and capacity to maintain micellization at lower concentrations. Meanwhile, the solutions of mixed micelles with various concentrations were irradiated by a red laser point to observe Tyndall phenomenon. As shown in Fig. 3B, blank PFP/PPP micelles demonstrated a light cross by irradiation and the light cross was fading with the dilution of blank PFP/PPP micelles. Low CMC suggests MIT-PFP/PPP micelles maintain self-assembly under diluted conditions which contributes to effective drug delivery. Furthermore, the stability of MIT-PFP/PPP micelles in the presence of FBS was evaluated. As shown in Fig. 3C, MIT-PFP/PPP micelles were stable in water

containing 10%, 20%, 30% and 40% FBS, which presented no significant size change to the low diameter ratio. The diameter ratios under all conditions were between 0.9 and 1.3, indicating that the particle size of MIT-PFP/PPP micelles changed in the range of 100 to 200 nm with good dispersibility. In addition, no visible particle precipitation was observed from MIT-PFP/PPP micelles dispersed in water with 10%, 20%, 30% and 40% FBS within 24 h (Fig. 3D).

3.3 *In vitro* release of MIT from mixed micelles

In vitro release profiles of MIT from MIT-PPP micelles and MIT-PFP/PPP micelles were obtained via dialysis. MIT is sensitive to light.[32] As shown in Fig. 2D, the accumulative release of MIT also decreased in the last 16 h. During the experiment of *in vitro* drug release, it was hard to avoid light completely, which may result in the loss of MIT to some extent and then lead to the decrease of accumulative release of MIT from mixed micelle in the last 16 h. The release of MIT from both MIT-PPP micelles and MIT-PFP/PPP micelles was lower than free MIT. Specifically, the cumulative release of free MIT reached 96% within 2 h, while cumulative release of MIT from MIT-PPP micelles and MIT-PFP/PPP micelles was 73% and 68%, respectively. After 4 h, both of MIT-PPP micelles and MIT-PFP/PPP micelles released over 80% of MIT, indicating that MIT released from mixed micelles occurred at a slower rate.

3.3 *In vitro* cytotoxicity

MTT assay was used to evaluate the cytotoxicity of free MIT, MIT-PPP micelles and MIT-PFP/PPP micelles against MCF-7 and MCF-7/ADR cells. As shown in Fig. 4, blank materials of PFP, PPP and PFP/PPP (1: 2) at the concentration of 50 μg/mL, which was higher than the concentration of blank materials used for forming MIT loaded mixed micelles, had no cytotoxicity on MCF-7 and MCF-7/ADR cells. The results indicated that MIT-PFP/PPP micelles provided better biocompatibility and enhanced the delivery of hydrophobic drugs into tumors.

Furthermore, MIT-PFP/PPP micelles showed higher cytotoxicity in both MCF-7

and MCF-7/ADR cells than free MIT and MIT-PPP micelles at various equivalent concentrations of MIT (Fig. 4). Table 1 showed the IC_{50} values of free MIT, MIT-PPP micelles and MIT-PFP/PPP micelles in both MCF-7 and MCF-7/ADR cells. The IC_{50} values of free MIT were 27.000±0.862 μM (24 h treatment) and 4.663±0.118 μM (48 h treatment) in MCF-7/ADR cells respectively, which were about 15-fold (1.735±0.190 μM) and 4.8-fold (0.966±0.041 μM) higher than that of free MIT in MCF-7 cells for 24 and 48 h, respectively. In MCF-7 cells, compared with the IC_{50} values of free MIT and MIT-PPP micelles, the MIT-PFP/PPP micelles had the lowest IC_{50} values of 1.058±0.152 μM (24 h treatment) and 0.519±0.043 μM (48 h treatment) respectively. In MCF-7/ADR cells, when MIT was encapsulated in PFP/PPP mixed micelle system, the IC_{50} value decreased by about 7.7-fold (3.503±0.163 μM) for 24 h treatment and decreased by about 4.7-fold (0.981±0.075 μM) for 48 h treatment compared to free MIT. Meanwhile, the IC_{50} of MIT encapsulated in PPP micelles was 1.31-fold (20.535±5.183 μM, 24 h treatment) lower than that of MIT in MCF-7/ADR cells respectively. These results suggest that PFP/PPP micelles potently reverse MDR in MCF-7/ADR cells.

Table 1. The IC_{50} values (μM) of free MIT, MIT-PPP micelles and MIT-PFP/PPP micelles in MCF-7 and MCF-7/ADR cells.

Formulation	MCF-7/ADR cells		MCF-7 cells	
	24 h	48 h	24 h	48 h
MIT	27.000±0.862	4.663±0.118	1.735±0.190	0.966±0.041
MIT-PPP micelles	20.535±5.183	4.940±1.660	1.4485±0.321	0.714±0.001
MIT-PFP/PPP micelles	3.5035±0.163	0.9815±0.075	1.058±0.152	0.519±0.043

3.4 Cellular uptake

Cellular uptake of chemotherapeutic drugs plays an important role in successful drug delivery.[33] However, overexpression of the efflux transporter P-gp in cancer cells hinders the delivery of therapeutic drugs. These membrane-bound pumps expel therapeutic drugs out of cells, leading to lower intracellular accumulation of drugs.[34] In this study, MIT-encapsulated micelles were found to inhibit the drug removal by

P-gp pumps and thus enhance the delivery and accumulation of MIT. The cellular uptake of MIT-PFP/PPP micelles was measured by flow cytometry in MCF-7/ADR cells. As shown in Fig. 5A, the accumulation of free MIT in MCF-7 cells was much higher than that in MCF-7/ADR cells, which suggested that the uptake of MIT was extruded out of MCF-7/ADR cells by efflux transporters. Interestingly, in MCF-7/ADR cells, the trend of increased accumulation of MIT released from MIT-PFP/PPP micelles was shown with the extension of incubation time, which was not present in MIT-PPP micelles as well as free MIT incubation. These results indicated that MIT-PFP/PPP micelles increased cellular uptake of MIT and enhanced the delivery of MIT.

3.5 Cell apoptosis

MIT is capable of inducing apoptosis in cancer cells.[35] Nuclear staining assay and Annexin V/PI dual staining assay were utilized to investigate the apoptotic activity of MIT in MCF-7/ADR cells. As shown in Fig. 5B, the untreated cells and cells treated with free MIT, MIT-PPP micelles, and MIT-PFP/PPP micelles were rounded without nucleus condensation after staining with hoechst fluorescent dye. This suggested that both free MIT and MIT-PPP micelles were unable to induce cell apoptosis in MCF-7/ADR cells. However, cells treated with MIT-PFP/PPP micelles were much less than the cells treated with free MIT and MIT-PPP micelles, which demonstrated that MIT-PFP/PPP micelles might inhibit the proliferation of MCF-7/ADR cells without inducing apoptosis.

To further confirm the anticancer effect of MIT-PFP/PPP micelles in MCF-7/ADR cells, Annexin V/PI staining was employed to analyze the early and late apoptotic cells. During cell apoptosis, Annexin V-FITC labels transmembrane phosphatidylserine of cancer cells and propidium iodide (PI) crosses the cell membranes due to increased membrane permeability.[36] As shown in Fig. 5C, few apoptotic cells (less than 10%) were observed after treatment with free MIT, MIT-PPP micelles and MIT-PFP/PPP micelles for 48 h, which was similar to untreated cells. These data indicated that both of free MIT and the corresponding formulations

(MIT-PPP micelles and MIT-PFP/PPP micelles) had no pro-apoptotic activity. Taken together, MIT-PFP/PPP micelles possessed anti-proliferation activity against MCF-7/ADR cells through inducing non-apoptotic pathway. This indicated that MIT anticancer effect might be associated with the molecular mechanism independent of apoptosis.

3.6 Western blot analysis

The development of MDR frequently correlates with overexpression of ATP-dependent membrane transporters in cancer cells, such as P-gp and MRP1, which pump out anticancer drugs from cancer cells.[37] To investigate whether the enhanced cytotoxic effect of MIT-PFP/PPP micelles is associated with P-gp expression level, western blot analysis was performed to evaluate the P-gp expression level, which is frequently overexpressed in drug-resistant cancer cells. In a previous study, it was reported that MIT could stimulate the protein expression of P-gp in cancer cells, which in turn resulted in multidrug resistant effect.[6] As shown in Figure 6, the expression of P-gp in MIT-treated MCF-7/ADR cells was obviously higher than that of untreated MCF-7/ADR cells. Once MIT was encapsulated in the core of PPP micelles, MIT-PPP micelles entered MCF-7/ADR cells mainly through endocytosis instead of P-gp transporters, which decrease the stimuli to P-gp expression. Thus, the protein expression level of P-gp has no obviously increase in MCF-7/ADR cells by MIT-PPP micelles compared to that of untreated cells. The MCF-7/ADR cells treated with MIT-PFP/PPP micelles showed the lowest P-gp expression level, suggesting that PFP/PPP micelles effectively down-regulated P-gp expression to reverse MDR in MCF-7/ADR cells.

4. Conclusion

In this study, a micelle system composed of various mixed ratios of PFP and PPP copolymers was optimized to encapsulate anticancer drug MIT to reverse MDR in human breast cancer cells. The MIT-PFP/PPP micelles were found to provide better biocompatibility, improving drug loading and cellular uptake with mono-dispersed

morphology. Moreover, MIT-PFP/PPP micelles exerted enhanced cytotoxicity effect against MCF-7 cells and MCF-7/ADR cells without inducing cell apoptosis, which may result from the suppression of P-gp mediated drug efflux by MIT-PFP/PPP micelles. Collectively, MIT-PFP/PPP micelles offer a promising approach to effectively delivering anticancer drugs despite MDR in cancer cells.

Acknowledgments

This study was supported by the Macao Science and Technology Development Fund (062/2013/A2), the Research Fund of the University of Macau (MYRG2014-00033-ICMS-QRCM, MYRG2014-00051-ICMS-QRCM, MYRG2015-00171-ICMS-QRCM), and the National Natural Science Foundation of China (81403120).

References

1. D. J. Taylor, C. E. Parsons, H. Han, A. Jayaraman and K. Rege, *BMC Cancer*, 2011, **11**, 470.
2. C. C. Cheng and R. K. Zee-Cheng, *Prog Med Chem*, 1983, **20**, 83-118.
3. D. Martincic and K. R. Hande, *Cancer Chemother Biol Response Modif*, 2005, **22**, 101-121.
4. L. R. Wiseman and C. M. Spencer, *Drugs Aging*, 1997, **10**, 473-485.
5. V. Martinez, O. Mir, J. Domont, D. Bouscary and F. Goldwasser, *Anticancer Drugs*, 2007, **18**, 233-235.
6. C. Nieth and H. Lage, *J Chemother*, 2005, **17**, 215-223.
7. J. D. Allen, A. van Loevezijn, J. M. Lakhai, M. van der Valk, O. van Tellingen, G. Reid, J. H. Schellens, G. J. Koomen and A. H. Schinkel, *Mol Cancer Ther*, 2002, **1**, 417-425.
8. K. Abu Ajaj, R. Graeser and F. Kratz, *Breast Cancer Res Treat*, 2012, **134**, 117-129.
9. K. Goda, F. Fenyvesi, Z. Bacso, H. Nagy, T. Marian, A. Megyeri, Z. Krasznai, I. Juhasz, M. Vecsernyes and G. Szabo, Jr., *J Pharmacol Exp Ther*, 2007, **320**, 81-88.
10. X. Li, P. Li, Y. Zhang, Y. Zhou, X. Chen, Y. Huang and Y. Liu, *Pharm Res*, 2010, **27**, 1498-1511.
11. C. Alvarez-Lorenzo, A. Sosnik and A. Concheiro, *Curr Drug Targets*, 2011, **12**, 1112-1130.
12. A. V. Kabanov, E. V. Batrakova and D. W. Miller, *Adv Drug Deliv Rev*, 2003, **55**, 151-164.
13. Y. Cai, Z. Sun, X. Fang, X. Fang, F. Xiao, Y. Wang and M. Chen, *Drug Deliv*,

2015, DOI: 10.3109/10717544.2015.1037970, 1-9.
14. Q. Zhou, Z. Zhang, T. Chen, X. Guo and S. Zhou, *Colloids Surf B Biointerfaces*, 2011, **86**, 45-57.
15. Z. Li and B. H. Tan, *Mater Sci Eng C Mater Biol Appl*, 2014, **45**, 620-634.
16. Y. Chen, X. Sha, W. Zhang, W. Zhong, Z. Fan, Q. Ren, L. Chen and X. Fang, *Int J Nanomedicine*, 2013, **8**, 1463-1476.
17. Z. Wei, J. Hao, S. Yuan, Y. Li, W. Juan, X. Sha and X. Fang, *Int J Pharm*, 2009, **376**, 176-185.
18. J. Zhang, Y. Li, W. Gao, M. A. Repka, Y. Wang and M. Chen, *Expert Opin Drug Deliv*, 2014, **11**, 1367-1380.
19. S. Wang, L. Wang, Z. Shi, Z. Zhong, M. Chen and Y. Wang, *PLoS One*, 2014, **9**, e97512.
20. S. Huang, X. Yu, L. Yang, F. Song, G. Chen, Z. Lv, T. Li, D. Chen, W. Zhu, A. Yu, Y. Zhang and F. Yang, *Eur J Pharm Sci*, 2014, **63**, 187-198.
21. S. Wang, R. Chen, J. Morott, M. A. Repka, Y. Wang and M. Chen, *Expert Opin Drug Deliv*, 2015, **12**, 361-373.
22. T. Yoshimura, K. Nyuta and K. Esumi, *Langmuir*, 2005, **21**, 2682-2688.
23. P. Opanasopit, T. Ngawhirunpat, A. Chaidedgumjorn, T. Rojanarata, A. Apirakaramwong, S. Phongying, C. Choochottiros and S. Chirachanchai, *Eur J Pharm Biopharm*, 2006, **64**, 269-276.
24. J. Zhang, Y. Li, W. Gao, M. A. Repka, Y. Wang and M. Chen, *Expert Opin Drug Deliv*, 2014, **11**, 1367-1380.
25. S. Tang, Q. Yin, J. Su, H. Sun, Q. Meng, Y. Chen, L. Chen, Y. Huang, W. Gu, M. Xu, H. Yu, Z. Zhang and Y. Li, *Biomaterials*, 2015, **48**, 1-15.
26. X. Zhao and P. Liu, *ACS Appl Mater Interfaces*, 2015, **7**, 166-174.
27. J. Zhang, M. Zhang, J. Ji, X. Fang, X. Pan, Y. Wang, C. Wu and M. Chen, *Pharm Res*, 2015, **31**, 3376-3390.
28. S. Wang, L. Wang, M. Chen and Y. Wang, *Chem Biol Interact*, 2015, **235**, 76-84.
29. M. Caldorera-Moore, G. N., S. L. and K. Roy, *Expert Opin Drug Deliv*, 2010, **7**, 479-495.
30. X. Y. Ke, N. V. W. Lin, S. J. Gao, Y. W. Tong, J. L. Hedrick and Y. Y. Yang, *Biomaterials*, 2014, **35**, 1096-1108.
31. J. Liu, Y. Pang, W. Huang, X. Zhu, Y. Zhou and D. Yan, *Biomaterials*, 2010, **31**, 1334-1341.
32. A. G. Bosanquet, *Cancer Chemother Pharmacol*, 1986, **17**, 1-10.
33. W. Jiang, B. Y. Kim, J. T. Rutka and W. C. Chan, *Nat Nanotechnol*, 2008, **3**, 145-150.
34. A. Krishan, C. M. Fitz and I. Andritsch, *Cytometry*, 1997, **29**, 279-285.
35. A. Koceva-Chyla, M. Jedrzejczak, J. Skierski, K. Kania and Z. Jozwiak, *Apoptosis*, 2005, **10**, 1497-1514.
36. S. Wang, T. Chen, R. Chen, Y. Hu, M. Chen and Y. Wang, *Int J Pharm*, 2012, **430**, 238-246.
37. R. Khonkarn, S. Mankhetkorn, M. Talelli, W. E. Hennink and S. Okonogi,

Colloids Surf B Biointerfaces, 2012, **94**, 266-273.

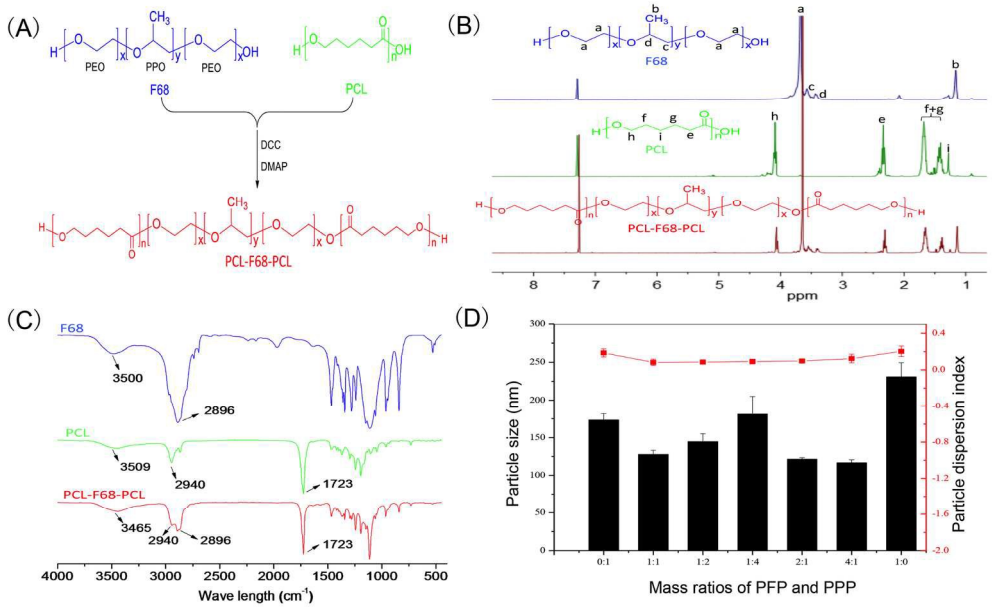

Fig. 1 (A) The synthetic pathway of PCL-F68-PCL (PFP); (B) 1H NMR spectrum of PCL-F68-PCL; (C) FTIR spectrum of PCL-F68-PCL; (D) The influence of different mass ratios of PFP and PPP used in MIT-PFP/PPP micelles on average particle size and particle dispersion index.
184x113mm (300 x 300 DPI)

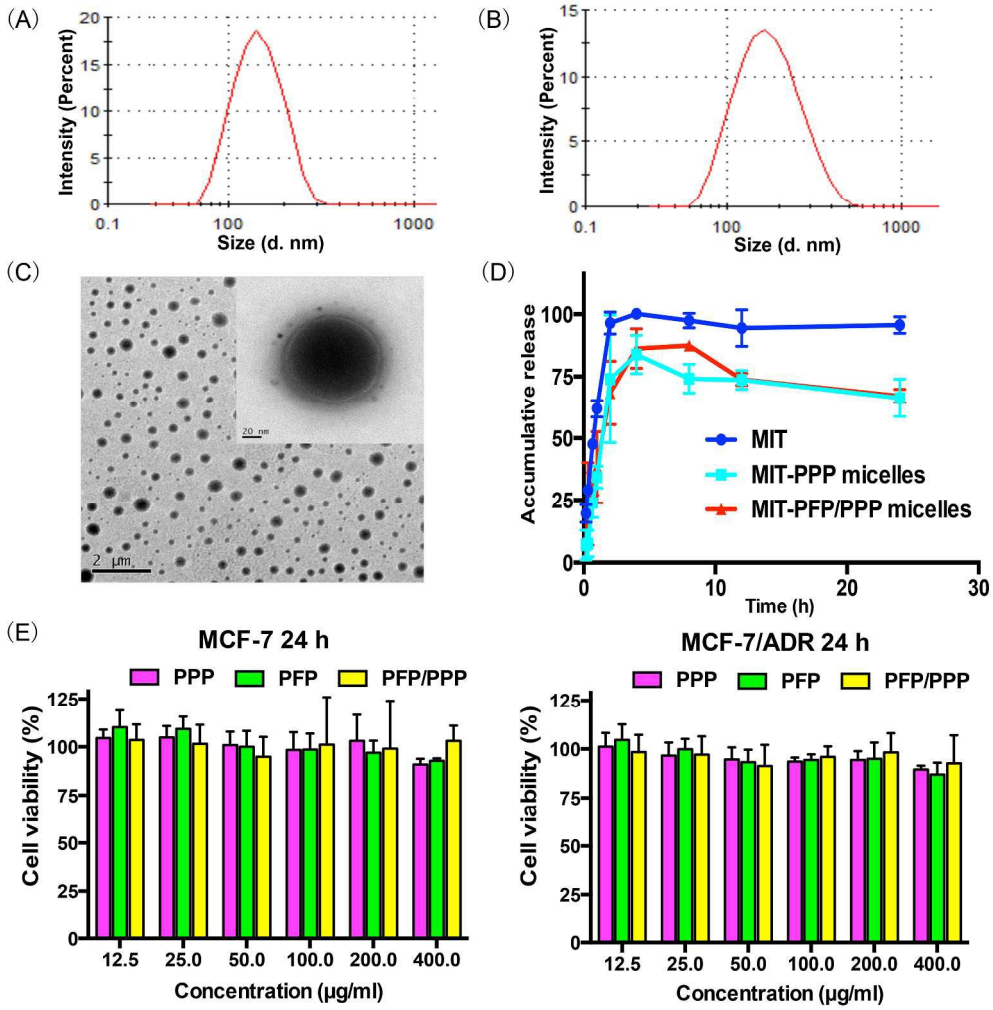

Fig. 2 (A) Size distribution of blank PFP/PPP (1: 2, w/w) micelles; (B) Size distribution of MIT-PFP/PPP (1: 2, w/w) micelles; (C) Transmission electron micrograph (TEM) of MIT-PFP/PPP (1: 2, w/w) micelles; (D) In vitro release profile of MIT from free MIT solution, MIT-PPP micelles and MIT-PFP/PPP micelles in phosphate-buffer saline (pH 7.4) containing 0.1% Tween 80 (v/v); (E) Cytotoxicity of PPP, PFP and PFP/PPP (1: 2, w/w) against MCF-7 and MCF-7/ADR cells.
295x299mm (300 x 300 DPI)

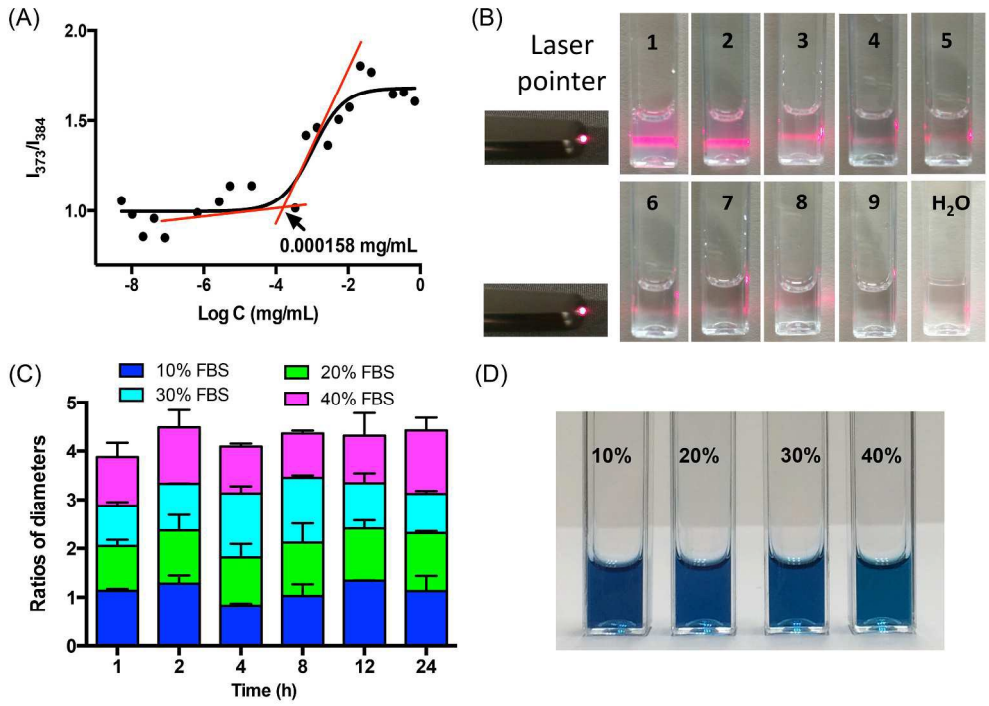

Fig. 3 (A) Critical micelle concentration (CMC) of blank PFP/PPP micelles using pyrene as a fluorescence probe; (B) Images of blank PFP/PPP micelles under the red laser irradiation by a laser pointer at various concentrations (1: 1.4; 2: 7×10-1; 3: 1.4×10-1; 4: 7×10-2; 5: 1.4×10-2; 6: 7×10-3; 7: 1.4×10-3; 8: 7×10-4; 9: 1.4×10-4 mg/mL); (C) Stability of MIT-PFP/PPP micelles in water containing 10%, 20%, 30% and 40% FBS during 24 h at 37ºC. The diameter ratio is the ratio between the hydrodynamic diameter at different time point and the initial diameter in water; (D) Photograph of MIT-PFP/PPP micelles after cultured with 10%, 20%, 30% and 40% FBS at 37ºC for 24 h.
294x212mm (300 x 300 DPI)

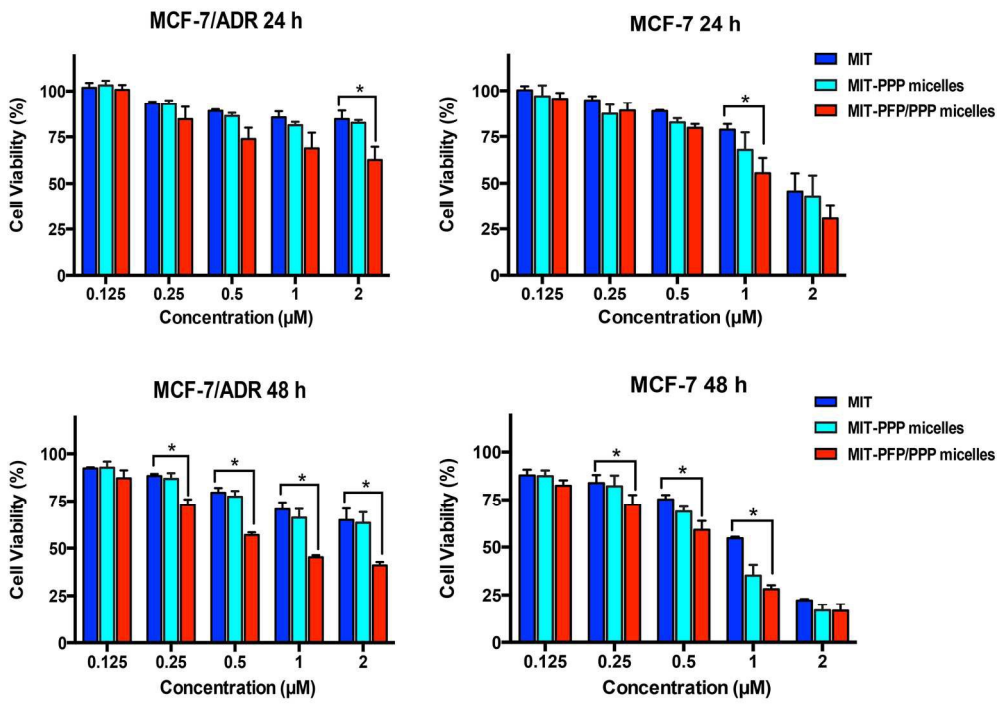

Fig. 4 Cell viability of MCF-7 and MCF-7/ADR cells after treatment with different concentrations of free MIT, MIT-PPP micelles and MIT-PFP/PPP micelles for 24 h and 48 h.
196x137mm (300 x 300 DPI)

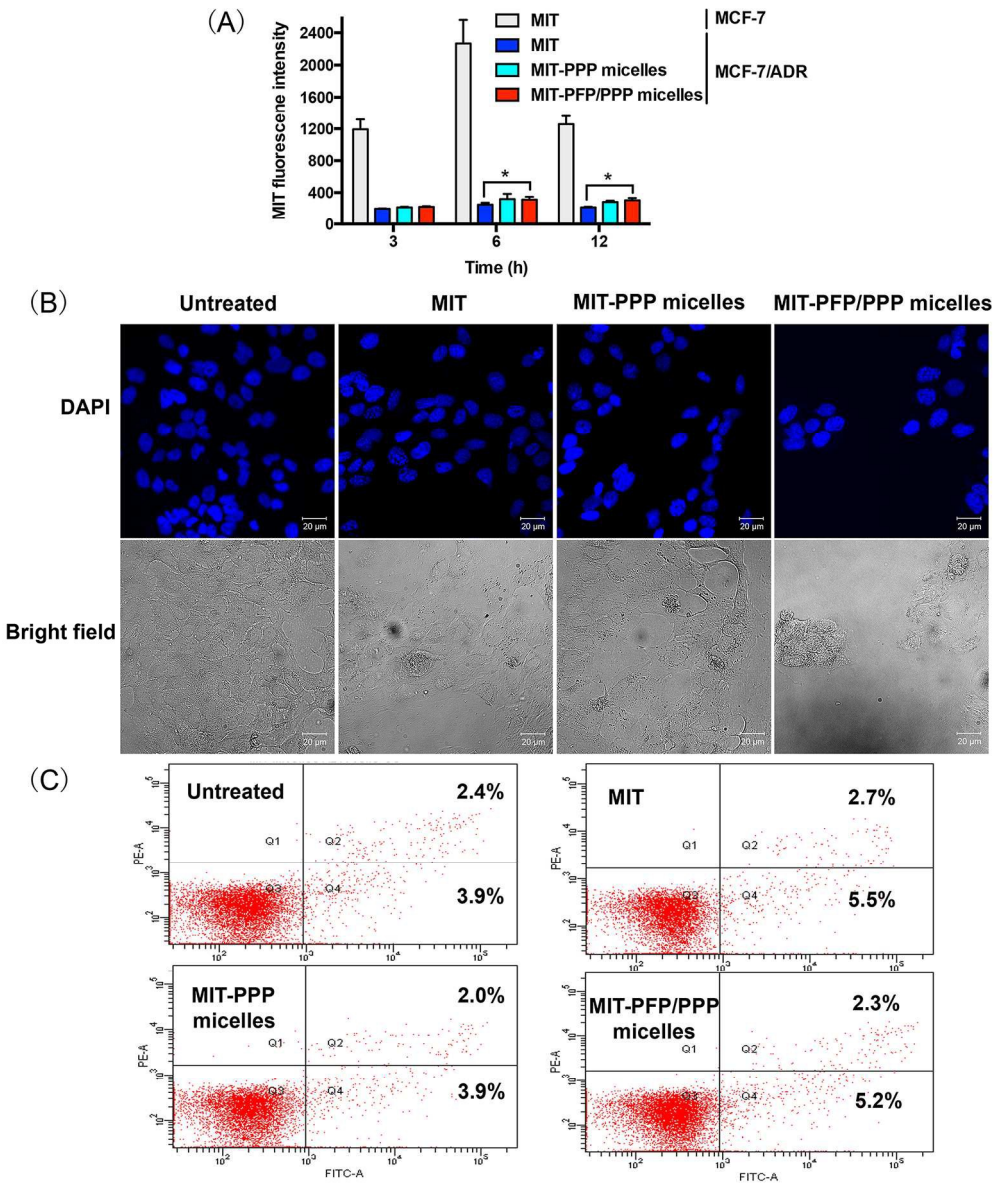

Fig. 5 (A) Flow cytometry analysis of intracellular uptake of MIT in MCF-7 cells and in MCF-7/ADR cells treated with free MIT, MIT-PPP micelles and MIT-PFP/PPP micelles at an equivalent concentration of MIT at 2 μM; (B) Nuclear morphology of MCF-7/ADR cells treated with free MIT, MIT-PPP micelles and MIT-PFP/PPP micelles at an equivalent concentration of MIT at 2 μM for 48 h. (C) Apoptosis analysis. MCF-7/ADR cells were treated as mentioned above and stained with Annexin V/PI followed by analysis via flow cytometry.
252x297mm (300 x 300 DPI)

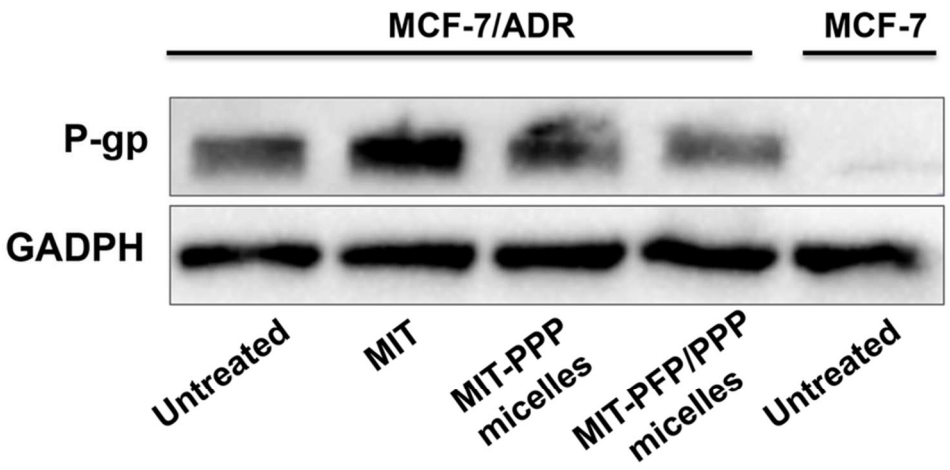

Fig. 6 Western blot analysis of P-gp expression in MCF-7/ADR cells treated with free MIT, MIT-PPP micelles and MIT-PFP/PPP micelles with an equivalent concentration at 2 μM for 48 h using the indicated antibodies.
78x39mm (300 x 300 DPI)

Graphical Abstract

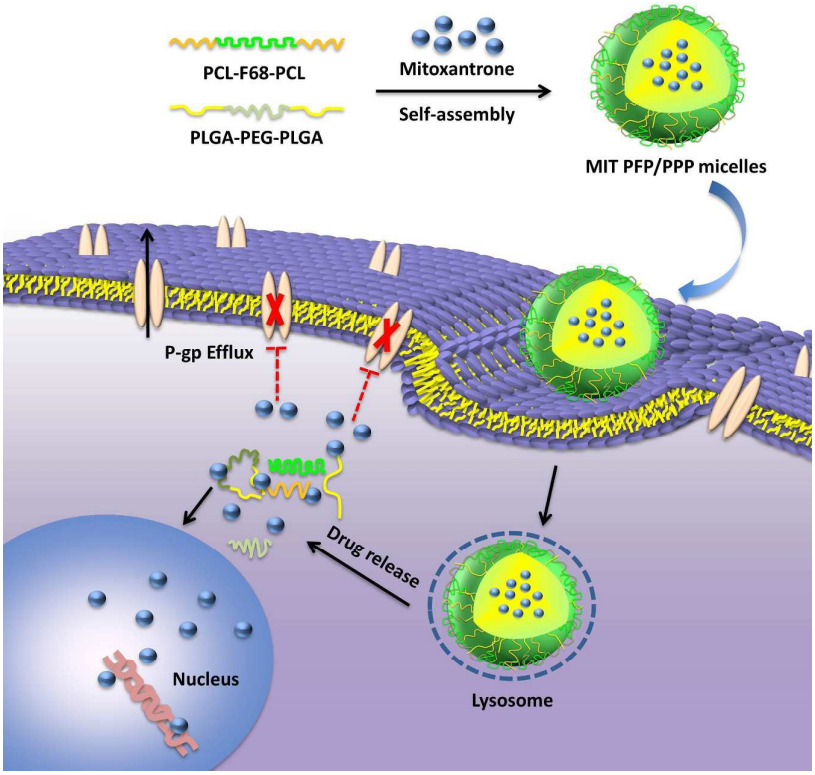

Scheme 1. Mitoxantrone-loaded PCL-F68-PCL/PLGA-PEG-PLGA mixed micelles for reversing multidrug resistant in breast cancer